

## Electronic structure, magnetism, and stability of Co-doped NiAl

D. J. Singh

Complex Systems Theory Branch, Naval Research Laboratory, Washington, D.C. 20375-5000

(Received 18 May 1992)

Total-energy and electronic-structure calculations for Co-doped NiAl are reported. The energy of a substitutional Co in NiAl is found to be approximately 11 mRy. For the doping levels considered (0–25% substitution on the transition-metal site) no evidence of structural instabilities or anomalies in elastic behavior is found. However, magnetic behavior is predicted for large Co concentrations. Strong nonrigid-band behavior is found for the doped system, and a high electronic density of states is associated with the Co atoms.

### I. INTRODUCTION

NiAl, CoAl, and related materials show potential for important aerospace applications<sup>1</sup> and as a result have been extensively studied, both experimentally and theoretically.<sup>2–12</sup> Both materials form in the bcc-derived CsCl structure, despite the fact that the constituent elements form in close-packed (fcc and hcp) structures. This, combined with the tendency toward ordering, the large heats of formation, the high melting temperatures, the deviations from Vegard's rule and theoretical work,<sup>7,11,12</sup> indicates the presence of substantial bonding in these materials.

Calculations have shown that the electronic structures of CoAl and NiAl are related by rigid-band behavior, differing primarily in the placement of the Fermi energy, which reflects the extra electron in NiAl, and in the

bandwidths. This is illustrated by the electronic densities of states (DOS's) for these materials, which are shown in Figs. 1 and 2. These were calculated using the general potential linearized augmented plane-wave (LAPW) method, as discussed below, and are similar to those obtained in earlier studies.<sup>7,8,10,11</sup> For both CoAl and NiAl, the DOS at the Fermi energy  $N(E_F)$  is relatively low. There is, however, a substantial peak in the DOS between the position of the Fermi energy in CoAl and that of NiAl. This peak suggests that if the electron count in NiAl were reduced, lattice instabilities or other anomalous behavior, such as magnetism or nonrigid-band behavior might result. In fact, if annealed, mixtures of NiAl and CoAl, tend to separate.<sup>13</sup> This and the effect of Co additions on the phase equilibria may be important in addressing the technologically important question of ductility improvement in NiAl-based alloys.<sup>14–17</sup> Here I investigate the more basic question of the effect of limited amounts of substitutional Co into NiAl.

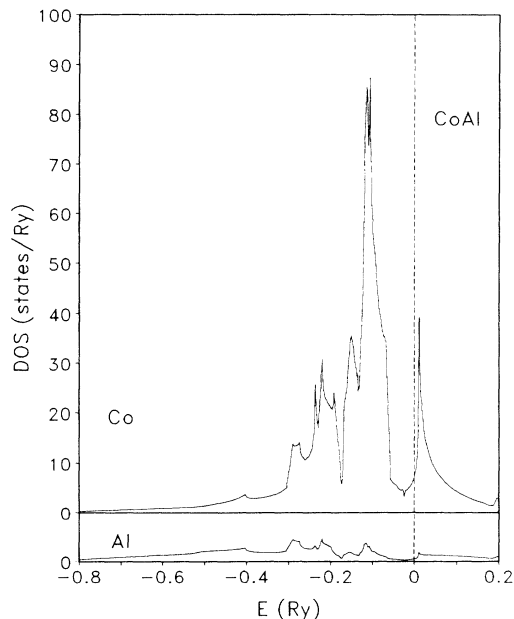


FIG. 1. Projected electronic DOS of CoAl at the calculated equilibrium lattice parameter. The dashed vertical line denotes the position of the Fermi energy. The projection is done by weighting each state by its contribution to the charge inside the Co and Al atomic spheres.

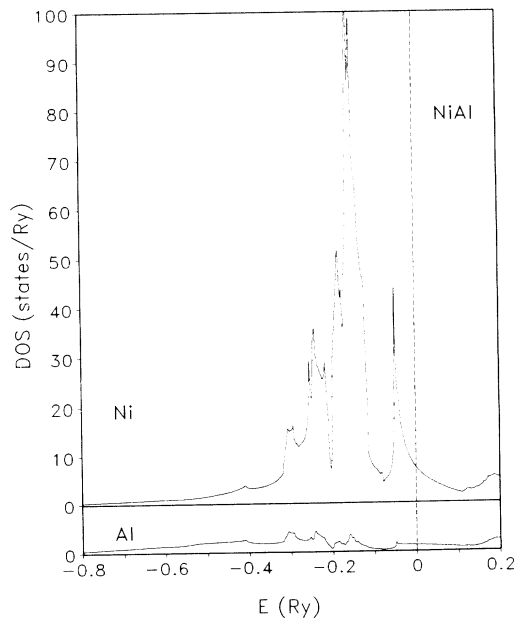


FIG. 2. Projected electronic DOS of NiAl at the calculated equilibrium lattice parameter. The dashed vertical line denotes the position of the Fermi energy.

## II. METHOD

The present calculations were performed, within the local (spin) density approximation [L(S)DA],<sup>18</sup> using the general potential linearized augmented plane-wave (LAPW) method,<sup>19</sup> with a local orbital extension<sup>20</sup> to relax the linearization of the narrow transition-metal-derived  $d$  bands. As mentioned, supercells were used to study the effect of Co substitution on the Ni sites. Besides calculations for NiAl and CoAl, which were used as references, calculations were performed for 8- and 16-atom supercells,<sup>21</sup> which correspond to 1:3 and 1:7 Co-to-Ni concentration ratios (i.e.,  $\text{Co}_{0.25}\text{Ni}_{0.75}\text{Al}$  and  $\text{Co}_{0.125}\text{Ni}_{0.875}\text{Al}$ , respectively). The 16-atom supercells were formed from a  $2 \times 2 \times 2$  arrangement of eight cubic NiAl cells with one Ni atom replaced by a Co atom. The 8-atom supercells were constructed by regarding this  $2 \times 2 \times 2$  arrangement of NiAl cells as a bcc structure and replacing one Ni atom on each of the bcc sublattices with a Co atom. In this 8-atom supercell (denoted 1:3 in the following) all the atoms are on symmetry sites and this facilitates the calculation of elastic constants. On the other hand, this supercell could not be used to calculate the structural relaxation around the Co atoms. In the 16-atom supercell (1:7 in the following) the nearest-neighbor shell of Al atoms could be relaxed, and total-energy calculations were used to study this. It may be noted that at a specific Co concentration there are infinitely more possible arrangements of the atoms than the simple ordered configurations considered here, and in general disorder can have substantial effects on materials properties. However, for low impurity concentrations, impurity-impurity interactions are weak and as a result the properties should not depend strongly on the particular configuration. The results (see below) for the two supercell sizes are similar, providing justification for the use of ordered supercells for the present study. In any case, the distribution of impurities is preparation dependent (note that NiAl and CoAl phase separate, so it is not sensible to consider the thermodynamic equilibrium distribution). While studying the distribution under particular conditions and its effects on the properties may be interesting, it is beyond the scope of the present study.

In the LAPW method space is divided into nonoverlapping atom-centered spheres and a remaining interstitial region. In the present calculations equal sphere radii of 2.15 a.u. were used for Al, Co, and Ni. Well-converged basis sets were used, corresponding to an interstitial plane-wave cutoff of 17.5 Ry, which yields approximately 100 LAPW basis functions per atom. The Brillouin zone samplings were performed using the special points technique.<sup>22</sup> Samplings of 56 special points in the irreducible wedge of the simple cubic zone were used in self-consistent calculations for CoAl and NiAl. In order to facilitate comparisons of the total energies, calculations for the 1:3 and 1:7 supercells were performed using the same  $\mathbf{k}$  points yielding 20 and 10 independent points, respectively, in the folded irreducible wedges. The elastic constants for the 1:3 supercell, however, were calculated using a slightly sparser mesh consisting of 14 special  $\mathbf{k}$

points in the irreducible wedge of the cubic Brillouin zone, which yields 45 and 42 inequivalent  $\mathbf{k}$  points for the orthorhombic and monoclinic strained lattices used to calculate  $c_{11}$ - $c_{12}$  and  $c_{44}$ , respectively.

## III. RESULTS AND DISCUSSION

### A. Energetics

Before investigating the electronic structures and searching for instabilities in Co-doped NiAl, a series of total-energy calculations was performed to investigate the feasibility of substituting Co for Ni in NiAl. In particular, the energies of the 1:3 and 1:7 supercells were calculated relative to the energies of separated NiAl and CoAl. The principal results of these calculations are summarized in Fig. 3, where the energies per Co atom of the various supercells are given relative to separated CoAl and NiAl. As mentioned, apart from adjustment of the lattice parameter, symmetry does not permit relaxing the structure of the 1:3 supercell. However, it is possible to symmetrically relax the distance of the nearest (to the Co substitutional) shell of Al atoms in the 1:7 supercell, and this was done. As shown in Fig. 3, the energy of the 1:3 supercell is calculated to be 11.0 mRy relative to separated NiAl and CoAl (note that this energy is for a non-spin-polarized system; the magnetic contribution to the energy is discussed below). The effective (i.e., per CsCl unit) equilibrium lattice parameter of the 1:3 supercell is found to be 5.345 a.u., which is intermediate between the calculated equilibrium lattice parameters of NiAl (5.368 a.u.) and CoAl (5.297 a.u.) and is very slightly smaller than would be predicted applying Vegard's rule to the pseudobinary. The energy of the 1:7 supercell is found to be 12.3 mRy higher than separated NiAl and CoAl without allowing relaxations. Although the lattice parameters of NiAl and CoAl are similar, a large relaxation could not be ruled out *a priori* because of the increased  $N(E_F)$ , which might be anticipated in the doped system. One manifestation of such a peak might be an anomalously large relaxation. In fact, as shown in Fig. 3, only a small inward relaxation of 0.013 Å of the nearest shell of Al atoms with a relaxation energy of only 0.8 mRy is found. This small relaxation provides an after-the-fact justification for not considering relaxations of further shells. Thus even including relaxation of the 1:7 supercell, its energy is higher than but close to that of the 1:3 supercell. These results imply that the effective Co-Co interaction in NiAl is attractive, corresponding to a tendency towards phase separation, and that the 11.5 mRy energy obtained from the 1:7 supercell is close to the energy of an isolated substitution in NiAl.

### B. Electronic Structure

As mentioned, if the electronic structure of the NiAl-CoAl pseudobinary were described by rigid-band behavior,  $N(E_F)$  would increase rapidly as Co is substituted for Ni in NiAl. In order to quantify this effect, consider reducing the electron count in the NiAl DOS or increasing

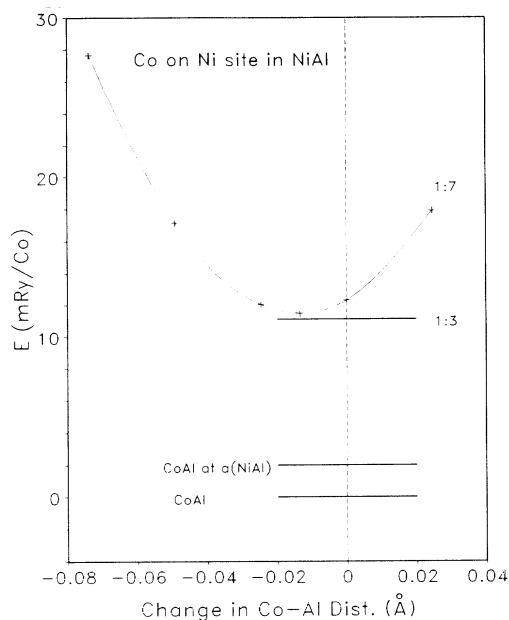


FIG. 3. Energetics of Co-doped NiAl relative to separated CoAl and NiAl. The horizontal bars labeled CoAl, CoAl at  $a(\text{NiAl})$ , and 1:3 are the relative energies per Co atom of CoAl at its equilibrium lattice parameter (0 by definition), CoAl strained to the NiAl lattice parameter, and the 1:3 supercell, respectively. The curve is a spline fit to calculated energies of the 1:7 supercell (calculated points are indicated by crosses) as a function of the nearest-neighbor Al relaxation.

it in the CoAl DOS. For a valence electron count of 12.75 (corresponding to the 1:3 alloy) the NiAl DOS is  $14.1 \text{ Ry}^{-1}$  and the CoAl DOS is  $14.7 \text{ Ry}^{-1}$ . For 12.875 electrons (corresponding to the 1:7 alloy) 12.2 and  $12.6 \text{ Ry}^{-1}$  are obtained from the NiAl and CoAl DOS, respectively. Evidence for nonrigid-band behavior would be values of  $N(E_F)$  outside the above ranges and differences between projections of the DOS on the Co and Ni sites. In fact this is the behavior of the 1:3 and 1:7 alloys.

The projected DOS's of the supercells, which are shown in Figs. 4 and 5, differ from the DOS of the end points and also the projections onto the Ni and Co sites differ significantly. These differences are reflected in the values of  $N(E_F)$ , which are given in Table I. It is remarkable that in the alloy system the Fermi energy falls near a peak in the projected DOS on the Co site and that the total  $N(E_F)$  of the 1:3 alloy is considerably higher than that which would be predicted from rigid-band behavior. This latter fact means that the nonrigid-band behavior cannot be rationalized as a consequence of the increasing DOS as the band filling in NiAl is reduced.

A clearer picture of the electronic structure can be obtained from a more detailed analysis of the DOS. First of all the projections of the DOS onto the Co site in the 1:3 and 1:7 alloys are quite similar. In both cases the band filling is essentially the same and is considerably larger than the band filling in CoAl (Fig. 1). This means that there is a substantial charge transfer from the Ni atoms to the Co atoms in the alloy. Second, the Co DOS in the

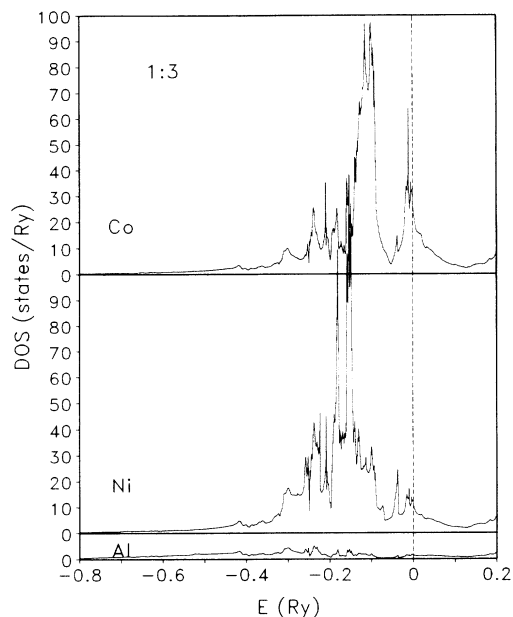


FIG. 4. Projected DOS of the 1:3 supercell from a non-spin-polarized calculation. The Ni and Al DOS are averages over the Ni or Al atoms in the cell. The dashed vertical line denotes the Fermi energy.

alloy is noticeably narrower than the Ni DOS. This is opposite to the behavior of the end points since the CoAl DOS is broader than the NiAl DOS. Further, the projections of the DOS onto the Ni sites in the alloys have widths which are similar to those in pure NiAl so that the main difference in the bandwidths is a narrowing of the Co  $d$  bands relative to CoAl. This band narrowing implies that the hybridization of the Co  $d$  orbitals with

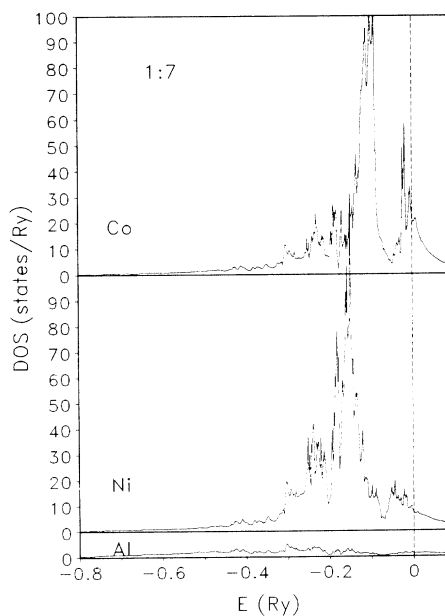


FIG. 5. Projected DOS of the relaxed 1:7 supercell. The Ni and Al DOS are averages over the Ni or Al atoms in the cell. The Fermi energy is denoted by the dashed vertical line.

TABLE I.  $N(E_F)$  in states/Ry for NiAl, CoAl, and the 1:3 and 1:7 supercells. The DOS are normalized to be per transition metal atom. The columns labeled Ni and Co are projections onto Ni and Co atomic spheres. The NiAl and CoAl and 1:3 supercells are at the calculated equilibrium lattice parameters. The calculation for the 1:3 supercell is non-spin polarized (see text). The 1:7 supercell is at the calculated NiAl lattice parameter and includes the nearest-neighbor relaxation around the Co impurity.

Material	Total	$N(E_F)$	
		Ni	Co
NiAl	10.8	7.3	
CoAl	8.9		7.2
1:3	19.7	11.0	27.8
1:7	12.5	7.3	22.0

those of neighboring transition-metal atoms (Ni in the alloy) is not as strong as in pure CoAl. Although at first sight this is surprising because of the fact the Co  $d$  orbitals may be expected to be more extended in the alloy (because of charge transfer to the Co site), it can be understood because the  $d$  orbitals of the neighboring Ni atoms will be less extended in the alloy for the same reason. Finally, in both the 1:3 and 1:7 supercells the projection on to the Co site has a two-peak structure similar to that in CoAl and NiAl and, in particular, the upper peak in the DOS, which lies between the position of the Fermi energies CoAl and NiAl, is quite prominent. On the other hand, the projections onto the Ni sites have reduced and broadened peaks. This leads to a much lower projection of  $N(E_F)$  on the Ni sites relative to the Co sites. While this could be due to changes in the hybridization, the absence of a comparable “smearing” of the Co DOS argues for an explanation in terms of crystal-field effects. I note that the charge transfer from the Ni to the Co sites means that there will be a substantial ionic component of the crystal field arising from the differing Ni (vs Co) occupations of the neighboring sites. For a Co atom in the 1:3 or 1:7 supercells for which calculations were performed, all the neighboring transition-metal sites are filled by Ni atoms. On the other hand, the Ni site symmetries are lower and in fact all the Ni atoms have at least one Co neighbor. This means that this ionic contribution to the crystal field will be small for the Co atoms but may be large for the Ni atoms, consistent with the “smearing” of the Ni DOS but not the Co DOS.

### C. Elastic behavior

As discussed above, the DOS's of the alloy systems are considerably higher than those of pure NiAl or CoAl, and it is frequently the case that an elevated DOS is associated with instabilities or anomalous properties. To investigate whether this is the case for the alloys, elastic constants were calculated and a search for ferromagnetism (see Sec. III D, below) was carried out.

Elastic constants were calculated for the reference alloys, NiAl and CoAl, as follows. The bulk modulus  $B$  was determined from fits to the Murnaghan<sup>23</sup> equation of

state of the total energies as a function of cell volume. The remaining two independent elastic constants were obtained by calculating the total energy as a function of volume conserving homogeneous strains and extracting the quadratic component of fits of these energies to polynomial forms as in Ref. 8, except that the calculations were performed at the calculated equilibrium volume instead of the experimental volume. Since the calculated equilibrium volumes are smaller than the experimental volumes (by 6.0 and 4.7 % in CoAl and NiAl, respectively), this leads to a stiffening of the elastic constants which, at least for these materials, degrades agreement with experiment. On the other hand, calculating elastic constants at the LDA lattice parameters permits calculations for systems such as the 1:3 alloy, for which experimental lattice parameters are not known, and thereby allows direct comparison of the results for the alloys with the end points in a search for anomalies. Further, this is a more truly first-principles procedure. Calculations for the 1:3 alloy were performed in the same way using identical strains. The results of these calculations are summarized in Table II. They show that in spite of the elevated DOS, the introduction of this level of Co into NiAl does not lead to anomalous elastic behavior. In fact, the elastic constants of the 1:3 alloy are not significantly different from those of pure NiAl. Although further work, particularly addressing slip behavior, is needed to draw firm conclusions, this result suggests that Co substitutions will not be effective in increasing the intrinsic ductility of near stoichiometric high-melting-temperature NiAl alloys.

Besides finding no anomalies in elastic behavior, the present calculations (see above) show that there is no anomalously large deviation from Vegard's law or large relaxation around the Co substitutional. It is known that there is a martensitic transformation in the  $Ni_xAl_{1-x}$  alloy system near  $x=0.62$ . The martensitic mode is strongly coupled to the same peak in the DOS which leads to the elevated DOS on the Co site in the CoAl-NiAl pseudo-binary considered here.<sup>10</sup> It is, however, unclear from the present results that substituting Co for Ni in NiAl moves the system closer to the martensitic instability. There is no evidence for it in the elastic constants of the 1:3 supercell calculated here. In view of the fact that a strain corresponding to  $c_{11}-c_{12}$  can transform the bcc-derived  $B2$  structure to a close-packed fcc-

TABLE II. Structural and elastic properties of NiAl, CoAl, and the 1:3 alloy. The elastic constants are at the calculated equilibrium lattice parameters. The properties for the 1:3 alloy are as obtained from non-spin-polarized calculations (see text). The lattice parameter given for the 1:3 alloy is the effective lattice parameter, i.e., half the bcc lattice parameter of the supercell.

	NiAl	Co <sub>0.25</sub> Ni <sub>0.75</sub> Al	CoAl
Lattice parameter (Å)	2.84	2.83	2.80
Bulk modulus (GPa)	185	188	204
$c_{11}$ (GPa)	262	274	341
$c_{12}$ (GPa)	146	145	136
$c_{44}$ (GPa)	138	131	165

derived structure, it is remarkable that even though Co substitutions increase the energy of the  $B2$  phase (see above), this shear elastic constant is not softened. This is, however, in accord with the results of Russell, Law, and Blackburn,<sup>15</sup> who found that for lower Al contents ( $x=0.64$ , which corresponds to the  $L1_0$  structure for NiAl), Co additions stabilize the  $B2$  structure at the expense of the martensite and the  $L1_0$  phase. This may be related to the strong nonrigid-band behavior which makes Co ineffective in elevating the projection of  $N(E_F)$  on the Ni sites and raises the open question of how well the elevated  $N(E_F)$  on the Co sites couples with the martensitic mode.<sup>10,24</sup>

#### D. Magnetism

For transition-metal systems it is often the case that elevated values  $N(E_F)$  are associated with magnetic instabilities. In order to investigate this, spin-polarized calculations were performed for the 1:3 and 1:7 supercells. For the 1:3 supercell, calculations were performed both at the calculated NiAl lattice parameter (5.368 a.u.) and that of the supercell (5.345 a.u., obtained from non-spin-polarized calculations). In both cases an instability against ferromagnetism was found. The moments in both cases were small. At the calculated lattice parameter the moment was  $0.49\mu_B$  with a magnetic energy of 1.4 mRy/Co atom, while at the NiAl lattice parameter the moment was  $0.58\mu_B$ /Co atom with a magnetic energy of 1.5 mRy/Co atom. In both cases, approximately two-thirds of the magnetization was contained within the Co spheres, with the remaining third being distributed among the neighboring Ni spheres. No ferromagnetic instability was found in calculations using the fixed spin moment procedure<sup>25</sup> for the larger 1:7 supercell, perhaps as a result of the lower  $N(E_F)$ . Thus the magnetic energy

acts to further lower the energy of the 1:3 supercell relative to the 1:7 supercell, strengthening the conclusion that the Co-Co impurity interaction in NiAl is attractive. Since the Co atoms in the 1:7 supercell are much more nearly isolated than those in the 1:3 supercell, it seems likely that the absence of magnetism in the larger supercell carries over to the case of a single impurity.

#### IV. CONCLUSIONS

LDA-based supercell calculations have been used to investigate the effect of substitutional Co in NiAl. The electronic structure is found to show strong nonrigid-band effects, and the development of a peak in the DOS which is associated with the substitutional Co atom. A supercell in which 25% of the Ni is replaced by Co is found to be ferromagnetic with a relatively low moment, even though neither NiAl nor CoAl nor a more dilute supercell is magnetic, and this may mean that magnetism can be used as a probe of the Co distribution in these alloys. No structural or elastic anomalies are found to correlate with the excess DOS associated with the Co sites. Only a small radial relaxation of the nearest-neighbor Al shell around a Co atom is found, and the calculated elastic constants are similar to those of pure NiAl. This is an indication that substitutional Co may not be effective in improving the intrinsic ductility of  $B2$ -structure NiAl.

#### ACKNOWLEDGMENTS

This work was supported by the Office of Naval Research. Computations were performed at the Cornell National Supercomputer Facility. I am pleased to acknowledge stimulating discussions with D. A. Papaconstantopoulos.

<sup>1</sup>See, for example, D. G. Backman and J. C. Williams, *Science* **255**, 1082 (1992), and references therein.

<sup>2</sup>V. L. Moruzzi, A. R. Williams, and J. F. Janak, *Phys. Rev. B* **10**, 4856 (1974).

<sup>3</sup>D. J. Nagel, Ph.D thesis, University of Maryland, 1977.

<sup>4</sup>R. Eibler and A. Neckel, *J. Phys. F* **10**, 2179 (1980).

<sup>5</sup>N. Stefanou, R. Zeller, and P. H. Dederichs, *Solid State Commun.* **59**, 429 (1986).

<sup>6</sup>B. I. Min, T. Oguchi, H. J. F. Jansen, and A. J. Freeman, *J. Magn. Magn. Mater.* **54-57**, 1091 (1986).

<sup>7</sup>S. C. Liu, J. W. Davenport, E. W. Plummer, D. M. Zehner, and G. W. Fernando, *Phys. Rev. B* **42**, 1582 (1990).

<sup>8</sup>M. J. Mehl, J. E. Osburn, D. A. Papaconstantopoulos, and B. M. Klein, *Phys. Rev. B* **41**, 10311 (1990); in *Alloy: Phase Stability and Design*, edited by G. M. Stocks, D. P. Pope, and A. F. Giamei, MRS Symposia Proceedings No. 186 (Materials Research Society, Pittsburgh, 1991), p. 277.

<sup>9</sup>Z. W. Lu, S. H. Wei, A. Zunger, S. Frota-Pessoa, and L. G. Ferreira, *Phys. Rev. B* **44**, 512 (1991).

<sup>10</sup>G. L. Zhao and B. N. Harmon, *Phys. Rev. B* **45**, 2818 (1992).

<sup>11</sup>T. Hong and A. J. Freeman, *Phys. Rev. B* **43**, 6446 (1991); *J. Mater. Res.* **7**, 68 (1992).

<sup>12</sup>C. L. Fu and M. H. Yoo, in *High Temperature Ordered Intermetallic Alloys IV*, edited by L. Johnson, D. P. Pope, and J.

O. Stiegler, MRS Symposia Proceedings No. 213 (Materials Research Society, Pittsburgh, 1991), p. 667.

<sup>13</sup>J. Schramm, *Z. Metallk.* **33**, 403 (1941); see also L. Kaufman and H. Nesor, *Metall. Trans. A* **6A**, 2123 (1975).

<sup>14</sup>A. Inoue, H. Tomioku, and T. Masumoto, *Metall. Trans. A* **14A**, 1367 (1983).

<sup>15</sup>S. M. Russell, C. C. Law, and M. J. Blackburn, in *High Temperature Ordered Intermetallic Alloys III*, edited by C. T. Liu, A. I. Taub, and N. S. Stoloff, MRS Symposia Proceedings No. 133 (Materials Research Society, Pittsburgh, 1989), p. 627.

<sup>16</sup>D. R. Pank, M. V. Nathal, and D. A. Koss, in *High Temperature Ordered Intermetallic Alloys III* (Ref. 15), p. 561.

<sup>17</sup>K. Ishida, R. Kainuma, N. Ueno, and T. Nishizawa, *Metall. Trans. A* **22A**, 441 (1991).

<sup>18</sup>The calculations were performed using the Hedin-Lundqvist exchange-correlation function with the spin-scaling of von Barth and Hedin; U. von Barth and L. Hedin, *J. Phys. C* **5**, 1629 (1972); L. Hedin and B. I. Lundqvist, *ibid.* **4**, 2064 (1971).

<sup>19</sup>S.-H. Wei and H. Krakauer, *Phys. Rev. Lett.* **55**, 1200 (1985); S.-H. Wei, H. Krakauer, and M. Weinert, *Phys. Rev. B* **32**, 7792 (1985), and references therein.

<sup>20</sup>D. Singh, *Phys. Rev. B* **43**, 6388 (1991).

<sup>21</sup>In units of  $2a$  the coordinates of the atoms in the simple cubic

16-atom supercell are Co: (0,0,0); Ni: (0.5,0,0), (0,0.5,0), (0,0,0.5), (0.5,0.5,0), (0.5,0,0.5), (0,0.5,0.5), (0.5,0.5,0.5); and Al: (0.25,0.25,0.25), (0.25,0.75,0.75), (0.75,0.25,0.75), (0.75,0.75,0.25), (0.75,0.75,0.75), (0.25,0.25,0.75), (0.25,0.75,0.25), (0.75,0.25,0.25). The 8-atom supercell is identical except that the Ni atom at (0.5,0.5,0.5) is replaced by a Co atom and the resulting bcc translational symmetry is used to divide the cell into two subcells.

<sup>22</sup>A. Baldereschi, *Phys. Rev. B* **7**, 5212 (1973); D. J. Chadi and M. L. Cohen, *ibid.* **8**, 5747 (1973); H. J. Monkhorst and J. D. Pack, *ibid.* **13**, 5188 (1976); **16**, 1748 (1977).

<sup>23</sup>F. D. Murnaghan, *Proc. Nat. Acad. Sci. U.S.A.* **30**, 244 (1944).

<sup>24</sup>Y. Noda, S. M. Shapiro, G. Shirane, Y. Yamada, and L. E. Tanner, *Phys. Rev. B* **42**, 10 397 (1990); Y. Yamada, Y. Noda, and K. Fuchizaki, *ibid.* **42**, 10 405 (1990).

<sup>25</sup>For the 1:7 alloy a series of fixed spin moment total-energy calculations was performed for magnetizations from 0 to  $0.5\mu_B/\text{cell}$ . The energy increased monotonically with the moment. For a description of the procedure, see, K. Schwarz and P. Mohn, *J. Phys. F* **14**, L129 (1984); see also, A. R. Williams, V. L. Moruzzi, J. Kubler, and K. Schwarz, *Bull. Am. Phys. Soc.* **29**, 278 (1984).